Probability Distributions of Local Liapunov Exponents for Small Clusters

Concezione Amitrano and R. Stephen Berry

The James Franck Institute and Department of Chemistry, The University of Chicago, 5735 South Ellis Avenue, Chicago, Illinois 60637

(Received 18 July 1991)

The probability distribution of the largest local Liapunov exponent is evaluated for a classical Ar_3 cluster at different values of the internal energy E, for a set of increasing values of the length in which the trajectory is partitioned. These distributions can be directly related to the evolution of ergodic behavior, particularly to how it exhibits distinctive, separable time scales which depend strongly on the energy of the system. Therefore, even though the inequivalence of ergodicity and chaos prohibits a Liapunov exponent itself from being a quantitative index of ergodicity, we find that *the sample distributions used to evaluate Liapunov exponents* nevertheless can be used for this purpose.

PACS numbers: 05.45.+b, 36.40.+d

The Ar_3 cluster has recently proved to be useful as a prototypical system in which to study details of phase changes in clusters, especially in the context of the question of how small systems explore their phase space [1-3]. The classical, conservative three-body Lennard-Jones system has been found to be chaotic even at low energies, where the power spectrum displays largely normal-mode structure. The degree of chaotic behavior as measured by the Kolmogorov entropy is nonzero at an energy corresponding to a mean temperature as low as 2 K. The K entropy increases with energy, then decreases sharply in the range of entry into and passage through the saddle regions of the linear configurations of the potential surface, and finally increases again at still higher energies [1].

At energies just high enough to allow passage over the linear saddle, the phase space seems to separate into a region of highly chaotic behavior that represents the motion in the well, and a region with much more "ordered" dynamics, that represents the motion across the saddle. In fact, above the transition energy the short-term average kinetic energy has a bimodal distribution that seems to correlate with the local values of the K entropy [1,3].

In previous work on the ergodicity of clusters, no examination was made of the systematic evolution from short-term to long-term behavior and only the statistic of global Liapunov exponents was examined. We suspected, as had others who used simple models as tests [4,5], that one could learn about this evolution by examining the probability distribution of the approximate values of the largest Liapunov exponent as a function of the duration of the interval used to obtain the time average, which is equivalent to the length of the averaging intervals into which the molecular-dynamic trajectory is partitioned. Those distributions make a powerful instrument to gain insight into the intriguing questions of the separation of phase space into high-chaos and low-chaos regions, and how the extent of ergodicity evolves in time for a few-body system.

To describe the classical Ar_3 cluster we take the Lennard-Jones Hamiltonian

$$H=\sum_{i=1}^{3}\frac{p_i^2}{2m}+4\epsilon\sum_{i<j}^{3}\left[\left(\frac{\sigma}{r_{ij}}\right)^{12}-\left(\frac{\sigma}{r_{ij}}\right)^{6}\right] \tag{1}$$

with $m=39.45$ amu, $\sigma=3.4$ Å, and $\epsilon=1.67\times10^{-14}$ erg. To generate the trajectories we use the following molecular-dynamics algorithm:

$$\mathbf{r}_i(t_n)=\mathbf{r}_i(t_{n-1})+\tau\mathbf{v}_i(t_{n-1})+\tfrac{1}{2}\tau^2\mathbf{a}_i(t_{n-1}), \tag{2a}$$

$$\mathbf{v}_i(t_n)=\mathbf{v}_i(t_{n-1})+\tfrac{1}{2}\tau[\mathbf{a}_i(t_n)+\mathbf{a}_i(t_{n-1})] \tag{2b}$$

(the velocity version of the Verlet algorithm [6]), with a time step $\tau=10^{-14}$ s, which makes one vibrational period correspond to 100-150 steps. In Eqs. (2), $\mathbf{r}_i$, $\mathbf{v}_i$, and $\mathbf{a}_i$ are the position, velocity, and acceleration of each argon atom, $i=1,2,3$. Initial conditions fix the center of mass and angular momentum at 0, and they remain constant during the simulation; the algorithm also conserves the total energy up to 1 part in 10^5-10^6 for millions of time steps. Finally, the temperature is simply defined through the equipartion theorem as the mean vibrational kinetic energy for the run.

As stated, our goal is to obtain and study the distributions of sample values of the largest Liapunov exponent on various time scales. For a d-dimensional space the local Liapunov exponents $\lambda_1^{(N)},\lambda_2^{(N)},\ldots,\lambda_d^{(N)}$ are calculated by propagating the Jacobian along the trajectory for $N-1$ steps, yielding

$$\{2^{\lambda_1^{(N)}},2^{\lambda_2^{(N)}},\ldots,2^{\lambda_d^{(N)}}\}=\left[\text{magnitude of eigenvalues of }\prod_{n=0}^{N-1}J(\mathbf{x}_n)\right]^{1/N}, \tag{3}$$

where $J(\mathbf{x}_n)$ is the Jacobian matrix of the propagators for each phase-space variable [7,8]. Of course, the Liapunov exponents would be found exactly by taking the limit $N \to \infty$. The largest Liapunov exponent quantifies the average divergence of two initially nearby trajectories for each time step, since repeated application of the Jacobian matrix turns an arbitrary vector in the direction of the eigenvector corresponding to the largest eigenvalue.

The algorithm for computing the Liapunov exponents involves calculating the Jacobian matrix at each time step, multiplying that matrix by the cumulative product of all the previous ones, and diagonalizing the final product after N time steps. Those eigenvalues are then converted to Liapunov exponents by taking their logarithm and dividing by N. This method, equivalent to that of Benettin, Galgani, and Strelcyn [9] in principle [10], has been verified in this work to be equivalent in practice also.

In the present case one is interested in calculating the largest Liapunov exponent $\lambda^{(N)} = \max_i \{\lambda_i^{(N)}\}$ for a set of increasing values of N. To speed our algorithm by saving matrix multiplications we limit ourselves to the following values of N: $\{2^i\}$, $i = 7,8,9,10,11,12,13$ or $N_i = \{128, 256, \ldots, 8192\}$, since for each of these values the product after N_i time steps can be obtained as the product of two N_{i-1} matrices.

Our simulations typically run for 10^9–10^{10} time steps (a total time of 10^{-5}–10^{-4} s), and start from a small number of different initial conditions that have already equilibrated. The distributions presented in this work contain from $\simeq 10^6$ sample values for trajectories of length 128 to $\simeq 10^5$ sample values of the Liapunov exponents for trajectories of length 8192, and no smoothing routine has been applied to them. Much shorter simulations ($\simeq 10^7$) were found to give the same qualitative amount of information, although the actual plots look much rougher and might need smoothing routines.

In Figs. 1(a)–1(d) we present our results for the energies $\{-1.394, -1.165, -0.939, \text{and } -0.792\} \times 10^{-14}$ erg per atom, corresponding to the mean vibrational temperatures $\langle T \rangle = 18.15$, 28.44, 30.65, and 36.71 K. To evaluate $\langle T \rangle$ we average the kinetic energy over the entire run, and then convert to temperatures; the results will be given without explicitly indicating the averaging, with the convention that temperatures always refer to long-time averages. In these pictures the distributions $g_{N_i}(\lambda)\, d\lambda$ [or the number of times λ was found in a bin of size 2.5×10^{-4} bits/$(10^{-14}$ s) for trajectories of length N_i] are plotted for $N_i = \{256, 512, \ldots, 8192\}$; the Liapunov exponents are given in bits/$(10^{-14}$ s). The area under each curve is proportional to the number of sample intervals for that

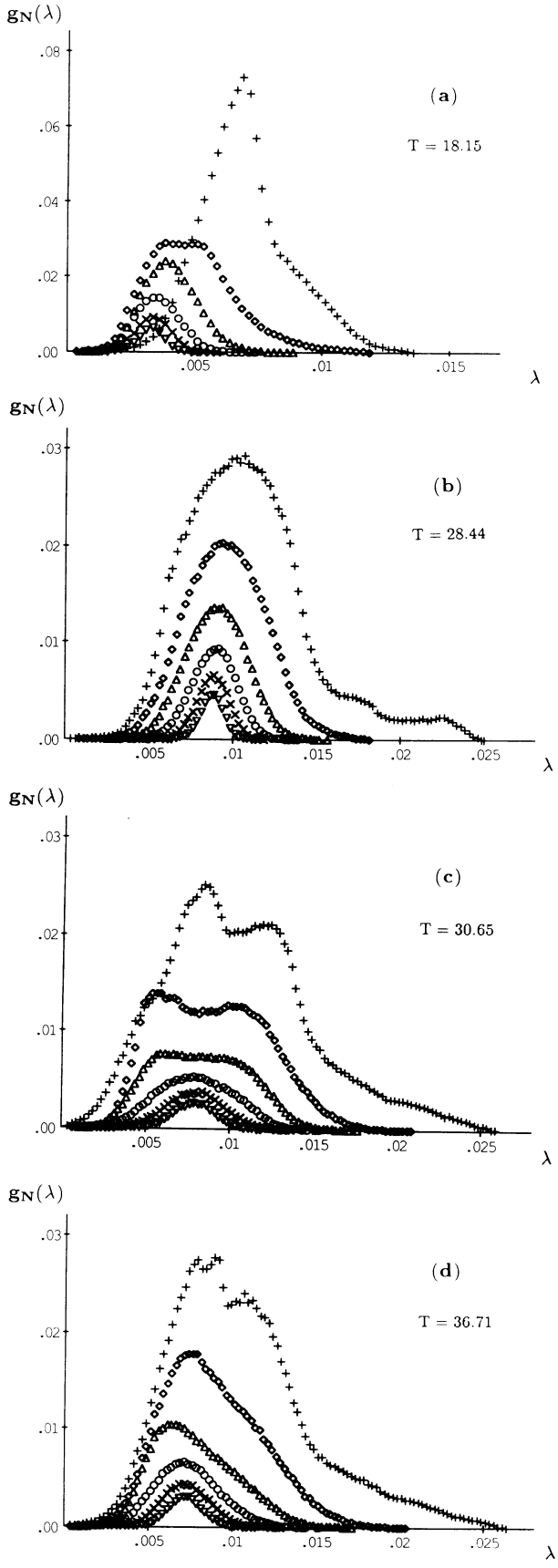

FIG. 1. $g_N(\lambda)$ vs λ at (a) $T = 18.15$ K, (b) $T = 28.44$ K, (c) $T = 30.65$ K, and (d) $T = 36.71$ K for $N = 256$ (+), $N = 512$ ($\diamond$), $N = 1024$ ($\triangle$), $N = 2048$ ($\circ$), $N = 4096$ ($\times$), and $N = 8192$ (∇). The units for λ are bits/$(10^{-14}$ s).

curve and the area under the curve $N_i=256$ is 1. The reason for using this normalization is mainly graphical (this way of plotting gives all the results at a glance), but also the scaling reflects the fact that in reality we have 2 times more data for the distribution g_{N_i} than for the distribution $g_{N_{i+1}}$.

We immediately see that the distributions for $T=18.15$ and 28.44 K are unimodal for any N_i, while for $T=30.65$ K there are two peaks for $N_i=256,512,1024$, and for $T=36.71$ K there are two well-defined peaks only for $N_i=256$. From previous work [1] we know that up to $\simeq T=28$ K the cluster has insufficient energy to penetrate the saddle regions, while at $T\geq 30$ K the cluster explores pathways over its three saddles around the equilateral minimum on the potential surface. Therefore our results are consistent with the interpretation of the phase space separating into a highly chaotic region with high kinetic energy and a much less chaotic region with high potential energy, and, in fact, at both $T=30.65$ and 36.71 K the Liapunov exponent distribution strongly correlates with the distribution of the short-term averages of kinetic energies. Of course, Fig. 1 also gives an estimate of the relative importance of the two regions. Moreover, we can see that while for $T=30.65$ K the separation of trajectories into trajectories that move in the high-chaos region and trajectories that move in the low-chaos region is meaningful up to trajectories of length $N_i=1024$, at $T=36.71$ K trajectories of length $N=512$ already overlap both regions.

Table I gives the average of the distribution for each curve. Whatever the temperature, λ shifts toward lower values with increasing N, implying that the asymptotic value for the largest Liapunov exponent can only be obtained by trajectories of more than 10^4 steps.

We would also like to point out that from our distributions we can easily derive the N approximation of the "spectrum of effective Liapunov exponents" [11] $\Phi_N(\lambda)=(1/N)\ln[P(\lambda_N;N)/P_{\max}(N)]$; plots of this quantity present a certain degree of data collapse with N, and will be discussed in a future publication.

Figure 2 shows a dramatic result concerning ergodicity. Here are two $N=256$ distributions for $\epsilon=-1.610\times10^{-14}$ erg per atom, $T=4.15$ K, whose only difference is the initial condition of the argon cluster. The distributions differ markedly, and show no tendency to converge over all the time scales we have probed, however long the run is. In fact, we have checked that the "shapes" of the distributions stay unaltered for tens of μs for all lengths of partitioning N_i. Moreover, the averages and the standard deviations of these distributions depend on the initial conditions for any N_i. Thus we conclude that at this temperature there is total nonergodicity up to at least tens of μs. In this case even averaging over 10^5 time steps will still only give a *local* Liapunov exponent [12,13].

We observe this nonergodicity up to $T\simeq16$ K: We have probed the energies $\{-1.526, -1.457,$ and $-1.429\}\times10^{-14}$ erg per atom, corresponding to the mean temperatures $T=10.10$, 14.56, and 16.13 K; again, all these distributions depend on the initial conditions. However, the higher the temperature, the smaller the dependence on the initial conditions; at $T=16.13$ K distributions derived from different initial conditions visually almost coincide, even though the average and standard deviations of the distributions are still different.

We have also evaluated the time autocorrelation function,

$$\Gamma_N(t)=\frac{\langle[\lambda_N(t)-\langle\lambda_N(t)\rangle][\lambda_N(0)-\langle\lambda_N(0)\rangle]\rangle}{\langle[\lambda_N(0)-\langle\lambda_N(0)\rangle]^2\rangle}, \qquad (4)$$

for the entire range of energies. At high energies, or energies corresponding to mean temperatures $T\geq18$ K, it appears that there are no long-time correlations even if the correlations at small values of N persist longer than the correlations at large values of N.

Instead at low temperatures the time autocorrelation function $\Gamma_N(t)$ shows long-time correlations, sometimes arranged in periodic patterns, and strongly dependent on the initial conditions. Figure 3 is an example of our results for the time correlations at $T=14.56$ K for the $N=256$ distribution and a particular but arbitrary choice of the initial conditions. We also give the time autocorre-

TABLE I. Average values of λ at $T=18.15$, 28.44, 30.65, and 36.71 K, for $N=128$, 256, 512, 1024, 2048, 4096, and 8192. The units are bits/$(10^{-14}$ s).

N	$T=18.15$	$T=28.44$	$T=30.65$	$T=36.71$
128	1.13×10^{-2}	1.63×10^{-2}	1.47×10^{-2}	1.59×10^{-2}
256	6.98×10^{-3}	1.09×10^{-2}	1.05×10^{-2}	1.05×10^{-2}
512	4.92×10^{-3}	9.58×10^{-3}	8.98×10^{-3}	8.84×10^{-3}
1024	4.08×10^{-3}	9.00×10^{-3}	8.29×10^{-3}	7.76×10^{-3}
2048	3.57×10^{-3}	8.83×10^{-3}	7.98×10^{-3}	7.34×10^{-3}
4096	3.36×10^{-3}	8.78×10^{-3}	7.89×10^{-3}	7.19×10^{-3}
8192	3.28×10^{-3}	8.76×10^{-3}	7.86×10^{-3}	7.14×10^{-3}

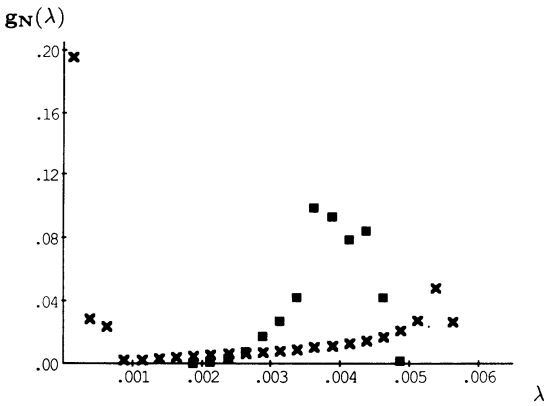

FIG. 2. $g_{256}(\lambda)$ vs λ at $T=4.15$ K for two different initial conditions.

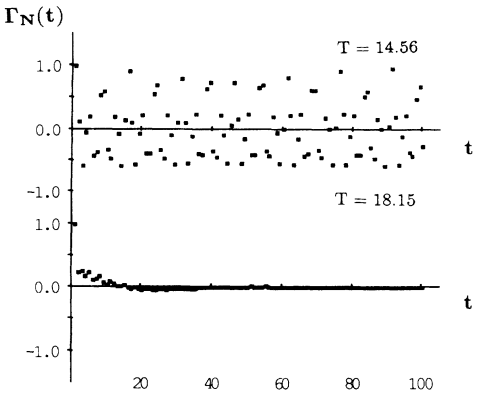

FIG. 3. $\Gamma_N(t)$ for $N=256$ at $T=14.56$ K and at $T=18.15$ K.

lation function at $T=18.15$ K for the same $N=256$ distribution, showing the normal fast decay to zero.

In conclusion, we have evaluated the distribution of the sample values of the largest Liapunov exponent for a classical Ar_3 cluster at different values of the total energy (and therefore of the mean temperature T), partitioning the trajectories into longer and longer intervals. At low energies, and even for the longest interval, the shape of the distribution depends on the initial conditions, a signature of the failure of the system to exhibit ergodicity even on long time scales. At intermediate energies the system is found to be ergodic with unimodal distribution of kinetic energies. At energies high enough to allow the system to pass into and across the saddle region separating local potential minima the distributions clearly show the separation of the phase space into a highly chaotic region with high kinetic energy and a much less chaotic region with high potential energy. These intermediate to high energy regions exhibit two time scales distinguishable by the change from bimodal to unimodal distribution of local Liapunov exponents; the shorter time scale is naturally that of lower ergodicity, and grows shorter with increasing energy.

These results show how a study of the *sample distributions* of Liapunov exponents, as they evolve from local to global, gives insight into how ergodicity evolves in time.

We would like to thank Itamar Procaccia and David Wales for useful discussions. This work was supported by Grant No. DE-FG02-86ER12488 from the Department of Energy. The simulations were done in part on the Cray-YMP at NCSA, Urbana, Illinois, whose support we also wish to acknowledge.

[1] T. L. Beck, D. M. Leitner, and R. S. Berry, J. Chem. Phys. **89**, 1681 (1988).
[2] D. M. Leitner, R. S. Berry, and R. M. Whitnell, J. Chem. Phys. **91**, 3470 (1989).
[3] D. J. Wales and R. S. Berry, J. Phys. B **24**, L351 (1991).
[4] J. P. Eckmann and I. Procaccia, Phys. Rev. A **34**, 659 (1986).
[5] M. A. Sepúlveda, R. Badii, and E. Pollak, Phys. Rev. Lett. **63**, 1226 (1989).
[6] D. W. Heermann, *Computer Simulation Methods* (Springer-Verlag, Berlin, 1986).
[7] P. Grassberger and I. Procaccia, Physica (Amsterdam) **13D**, 34 (1984).
[8] D. Ruelle and J-P. Eckmann, Rev. Mod. Phys. **57**, 617 (1985).
[9] G. Benettin, L. Galgani, and J-M. Strelcyn, Phys. Rev. A **14**, 2338 (1976).
[10] A. Wolf, J. B. Swift, H. L. Swinney, and J. A. Vastano, Physica (Amsterdam) **16D**, 285 (1985).
[11] P. Grassberger, R. Badii, and A. Politi, J. Stat. Phys. **51**, 135 (1988).
[12] M. Casartelli, Nuovo Cimento B **76**, 97 (1983).
[13] M. C. Carotta, C. Ferrario, G. Lo Vecchio, and L. Galgani, Phys. Rev. A **17**, 786 (1978).